Molecular Biology of the Cell
Vol. 14, 4984–4996, December 2003

The Adaptor Protein ARH Escorts Megalin to and through Endosomes

Masaaki Nagai,* Timo Meerloo,* Tetsuro Takeda,* and Marilyn Gist Farquhar*†‡

Departments of *Cellular and Molecular Medicine and †Pathology, University of California, San Diego, La Jolla, California 92093

Submitted June 10, 2003; Revised August 8, 2003; Accepted August 18, 2003
Monitoring Editor: Juan Bonifacino

Megalin is an endocytic receptor that binds multiple ligands and is essential for many physiological processes such as brain development and uptake of proteins by the kidney tubule, yolk sac, and thyroid. The cytoplasmic tail of megalin contains two FXNPXY motifs. Autosomal recessive hypercholesterolemia (ARH) is an adaptor protein that binds to the FXNPXY motif of the low-density lipoprotein receptor as well as clathrin and AP-2. We found that ARH also binds to the first FXNPXY motif of megalin in two-hybrid, pull-down and coimmunoprecipitation assays. ARH colocalizes with megalin in clathrin coated pits and in recycling endosomes in the Golgi region. When cells are treated with nocodazole, the recycling endosomes containing megalin and ARH disperse. On internalization of megalin, ARH and megalin are first seen in clathrin coated pits followed by sequential localization in early endosomes and tubular recycling endosomes in the pericentriolar region followed by their reappearance at the cell surface. Expression of ARH in Madin-Darby canine kidney cells expressing megalin mini-receptors enhances megalin-mediated uptake of ^{125}I-lactoferrin, a megalin ligand. These results show that ARH facilitates endocytosis of megalin, escorts megalin along its endocytic route and raise the possibility that transport through the endosomal system is selective and requires interaction with specific adaptor proteins.

INTRODUCTION

Megalin, like other members of the low-density lipoprotein receptor (LDLR) gene family, is an essential endocytic receptor expressed in clathrin-coated pits that continually internalizes bound ligands by receptor-mediated endocytosis. Megalin is unique among LDLR family members in that it is found at the apical plasma membrane of numerous epithelia, including those of the kidney proximal tubule (Kerjaschki and Farquhar, 1983; Chatelet *et al*., 1986), lung (type II cells), thyroid, yolk sac, and epididymis (Zheng *et al*., 1994). Megalin specifically binds and takes up a large variety of proteins, including albumin, polypeptide hormones, apolipoproteins, lactoferrin, vitamins carriers, polybasic drugs, receptor-associated protein (RAP), and Sonic hedgehog (Shh), a secreted signaling molecule (Farquhar *et al*., 1995; Christensen *et al*., 1998; Orlando *et al*., 1998; Christensen and Willnow, 1999; McCarthy *et al*., 2002). That megalin has crucial functions is demonstrated by the fact that megalin knockout mice have defective forebrain development, defects in pulmonary function, and altered kidney function (Willnow *et al*., 1996; Christensen *et al*., 1998; Christensen and Willnow, 1999; Nykjaer *et al*., 1999).

It has become evident that selective endocytic uptake of ligands is mediated by binding of signals in the cytoplasmic tails of receptors to cytoplasmic adaptor proteins. There are a growing number of both signals and adaptor proteins that function along the endocytic pathway (Bonifacino and Traub, 2003). Thus, the regulation of a receptor's unique function in endocytosis, sorting, and signaling is mediated through interactions of its cytoplasmic tail. Megalin has a 213-amino acid cytoplasmic tail (Saito *et al*., 1994) with little sequence similarity to other LDLR family members except for FXNPXY motifs, the first sorting signal discovered (Davis *et al*., 1986; Chen *et al*., 1990). The cytoplasmic tail of megalin contains two such FXNPXY motifs and one similar NXXY motif (Saito *et al*., 1994). It also contains a putative di-leucine-based sorting signal and binding motifs for SH2, SH3, and PDZ (PSD-95/Dlg/ZO-1) domains through which it binds to multiple intracellular adaptor proteins involved in sorting and signaling (May *et al*., 2003). These include Dab2 (Oleinikov *et al*., 2000), which interacts with the second FXNPXY motif, MAGI-I (Patrie *et al*., 2001) and GIPC (Gotthardt *et al*., 2000; Lou *et al*., 2002), which bind to the C-terminal PDZ binding motif (DSDV), and ANKRA (Rader *et al*., 2000) and MegBP (Petersen *et al*., 2003), which interact with the juxtamembrane proline-rich motif. The effects of these adaptor proteins on megalin endocytosis and signaling are still unclear.

Recently, a novel adaptor protein, ARH, a phosphotyrosine binding (PTB) protein (Yan *et al*., 2002), was identified based on mutations in a subset of patients with autosomal recessive familial hypercholesterolemia (ARH) (Garcia *et al*., 2001). Patients who are homozygous for a defect in this gene fail to internalize low-density lipoprotein (LDL) in the liver and exhibit severe hypercholesterolemia and premature coronary heart disease, implying that ARH is required for efficient uptake of LDL. Further work has established that ARH binds to clathrin, adaptor protein (AP)-2, and phos-

Article published online ahead of print. Mol. Biol. Cell 10.1091/mbc.E03–06–0385. Article and publication date are available at www.molbiolcell.org/cgi/doi/10.1091/mbc.E03–06–0385.

‡ Corresponding author. E-mail address: mfarquhar@ucsd.edu.

phoinositides as well as to FXNPXY motifs (He *et al*., 2002; Mishra *et al*., 2002b), but the precise site of localization of this protein and its role in endocytosis are still unclear. In some tissues, such as kidney and placenta, ARH is highly expressed and LDLR expression is relatively low (Garcia *et al*., 2001), raising the possibility that ARH might have other binding partners.

In this study, we provide evidence that ARH binds to the first FXNPXY sequence in the cytoplasmic tail of megalin as well as the FXNPXY sequence of LRP and that ARH accompanies megalin throughout its intracellular recycling itinerary from clathrin coated pits (CCPs), to and through early endosomes and recycling endosomes, and back to the cell surface. Surprisingly, it also facilitates transport of megalin through the endosomal system.

MATERIALS AND METHODS

Redivue [^{35}S]methionine (>1000 Ci/mmol) was purchased from Amersham Biosciences (Piscataway, NJ) and Na[^{125}I] (100 mCi/ml) from PerkinElmer Life Sciences (Boston, MA). Primers were synthesized by GenBase (San Diego, CA), and restriction enzymes were from New England Biolabs (Beverly, MA). Human full-length LDLR and LDLR-related protein (LRP) cDNA were obtained from Dr. Joachim Herz (University of Texas, Austin, TX) and used as a template for the polymerase chain reaction (PCR). Enhanced chemiluminescence substrate (SuperSignal) was obtained from Pierce Chemical (Rockford, IL). Chemical reagents were obtained from Sigma-Aldrich (St. Louis, MO) except as indicated. The expressed sequence tag (EST) of human ARH was purchased from the IMAGE Consortium (ResGen, Huntsville, AL).

Antibodies

Polyclonal rabbit anti-megalin (LBD IV) (Yamazaki *et al*., 1998), mouse anti-megalin mAb 20B against the ectodomain of megalin (Miettinen *et al*., 1990), and polyclonal rabbit anti-α-mannosidase II (Velasco *et al*., 1993) were prepared as described previously. Affinity-purified rabbit anti-syntaxin 13 IgG was obtained from Dr. Rytis Prekeris (University of Colorado, Boulder, CO) and anti-transferrin receptor (H68.4) mAb was from Dr. Ian Trowbridge (Salk Institute, San Diego, CA). Anti-AP-2/α-adaptin mAb was purchased from Affinity Bioreagents (Golden, CO), anti-EEA1 and anti-Rab11 mAbs were from BD Biosciences (San Diego, CA), and anti-FLAG (M2) from Sigma-Aldrich. Cross-absorbed Alexa 488-conjugated goat anti-rabbit F(ab')$_2$ and Alexa 594-conjugated goat anti-mouse F(ab')$_2$ were purchased from Molecular Probes (Eugene, OR). Affinity-purified goat anti-rabbit and anti-mouse IgG-horseradish peroxidase conjugates were from Bio-Rad (Hercules, CA).

Antisera against rat ARH were raised in rabbits against the purified glutathione *S*-transferase (GST)-tagged C terminus (aa 170–299) of rat ARH and affinity purified on GST-ARH coupled to CNBr Sepharose 4B beads (Amersham Pharmacia AB, Uppsala, Sweden).

Yeast Two-Hybrid Screening

The rat megalin partial cDNA (Saito *et al*., 1994) and construction of the rat cDNA library (Takeda *et al*., 2001) were described previously. The cDNA encoding the N-terminal part of the cytoplasmic domain of rat megalin (aa 4423–4558) (includes the first FXNPXY and NXXY motifs) was amplified by PCR and inserted into the *Eco*RI and *Xho*I sites in the LexA DNA binding domain of the bait vector (Display System Biotech, Vista, CA). The resulting vector, pBAIT-MT, and the reporter vector (containing the green fluorescent protein gene as a reporter) were transformed in yeast strain EGY48 (Invitrogen, Carlsbad, CA).

For interaction screening in the LexA-based version of the yeast two hybrid system, 20 μg of the rat cDNA library in the prey vector was transformed in the yeast that had been pretransformed with pBAIT-MT and reporter vectors. Yeast transformants (3.6×10^5) were plated onto selective medium (−histidine, −uracil, −leucine, −tryptophane, −glucose, +galactose), and colonies that survived were exposed to standard UV light (360 nm). Plasmid DNA from the positive colonies was rescued by electroporation into *Escherichia coli* KC8 (BD Biosciences Clontech, Palo Alto, CA). Both strands of the DNA inserts were sequenced by automated sequencing (Molecular Pathology Shared Resource, University of California San Diego Cancer Center). BLAST searches were performed via the Web site of the National Center for Biotechnology Information (Altschul *et al*., 1990).

cDNA Cloning

To obtain the complete coding sequence for rat ARH, 5′ rapid amplification of cDNA ends (RACE) was performed on the same rat cDNA library. The RACE product was ligated into pPCR-Script Amp SK(+) vector (Stratagene, La Jolla, CA) and sequenced on both strands.

One-to-One Interactions in the Yeast Two-Hybrid System

Fragments of the cytoplasmic tail of megalin, LRP, and LDLR were generated by PCR. For mapping interaction sites, regions of the cytoplasmic tails and rat ARH were subcloned into the *Eco*RI and *Xho*I sites of the bait and prey vectors, respectively. Bait and prey constructs were cotransformed into yeast strain EGY48 with the reporter vector. Transformants were plated onto selective medium and colonies that survived were exposed to standard UV light.

In Vitro Pull-Down Assays

The cDNA encoding the cytoplasmic domain of rat megalin (aa 4423–4635) was amplified by PCR and inserted into pGEX-KG (Amersham Pharmacia AB), and GST fusion proteins or GST alone were expressed in BL 21 (DE3), purified, and immobilized on glutathione-agarose beads (Amersham Pharmacia AB). ^{35}S-Labeled rat ARH was produced using the TNT T7 rabbit reticulocyte quick coupled transcription/translation system (Promega, Madison, WI) in the presence of [^{35}S]methionine and pCDNA3-rat ARH constructs. In vitro-translated products were incubated with 5 μg of GST-megalin cytoplasmic tail (GST-MT) or GST alone immobilized on glutathione-agarose beads in binding buffer (20 mM HEPES, pH 7.4, 150 mM NaCl, 2 mM $CaCl_2$, 10 mM CHAPS, 1 mM dithiothreitol, 0.1% bovine serum albumin [BSA], and 10 μg/ml leupeptin) for 15 h at 4°C with gentle rocking. Bound proteins were eluted with 25 μl Laemmli sample buffer, resolved by 12.5% SDS-PAGE, and visualized by autoradiography with Biomax MR x-ray film (Eastman Kodak, Rochester, NY).

Cell Culture

Madin-Darby canine kidney (MDCK) and L2 yolk sac cells were maintained in minimal essential medium Earle's or DMEM Hi-glucose, respectively, supplemented with 10% fetal calf serum and 100 U/ml penicillin G and 100 μg/ml streptomycin sulfate (Invitrogen) at 37°C and 5% CO_2. MDCK-M4 cells which stably express megalin mini-receptors (Takeda *et al*., 2003) were maintained in minimal essential medium Earle's with 0.8 mg/ml genetecin (Invitrogen) and 0.25 mg/ml zeocin (Invitrogen).

Generation of MDCK-M4 Cells Expressing ARH

The N-terminal FLAG-tag construct was added to the pMSCVpuro retroviral vector (BD Biosciences), by inserting the ds-oligonucleotides encoding the FLAG epitope (DYKDDDDK) into the *Xho*I and *Eco*RI sites of pMSCVpuro. Full-length and the N terminus (aa 1–178) of human ARH were generated by PCR by using the human EST as template, and these PCR fragments were subcloned into the *Eco*RI site of N-terminal FLAG-pMSCVpuro (pMSCV-ARH and pMSCV-N′ARH, respectively).

High-titer, helper-free retrovirus was prepared by transient transfection of human embryonic kidney (HEK)293T cells using the *kat* ecotropic packaging system (Finer *et al*., 1994). HEK293T cells were transfected with the respective retroviral construct (pMSCV-ARH, pMSCV-N′ARH and retrovirus vector alone) together with a packaging construct (pKat2, provided by Dr. Mark Kamps, University of California San Diego) using calcium phosphate. Supernatants were collected 48 h after transfection and passed through a 0.45-μm filter before freezing at −80°C. MDCK-M4 cells were infected with supernatant containing retrovirus with 8 μg/ml polybrene and were selected in 3.5 μg/ml puromycin 48 h postinfection. Selected cell lines were named MDCK-M4-ARH, MDCK-M4-N′ARH, and MDCK-M4-mock, respectively.

Preparation of Cell and Tissue Lysates for Immunoblotting

Cells and tissue fragments were lysed in lysis buffer (0.5% Triton X-100, 20 mM Tris-HCl, pH 7.4, 150 mM NaCl, and 1 mM EDTA) containing protease inhibitors (10 μg/ml leupeptin and 0.5 mM phenylmethylsulfonyl fluoride). Proteins were boiled for 5 min in Laemmli sample buffer supplemented with 5%, 2-mercaptoethanol, separated on 12.5% SDS-PAGE, and transferred to polyvinylidene difluoride membranes (Millipore, Bedford, MA). Membranes were blocked (1 h in phosphate-buffered saline, pH 7.2, containing 5% calf serum, and 0.1% Tween 20), incubated for 2 h at 25°C with primary antibodies, followed by horseradish peroxidase-conjugated goat anti-rabbit IgG (1 h, 1:3000 dilution) and detection by enhanced chemiluminescence.

Immunoprecipitation

MDCK-M4-ARH and MDCK-M4-mock cells were seeded (5×10^6 cells) on 100-mm dishes, grown for 2 d to reach confluence, lysed with 500 μl of lysis buffer (0.5% Triton X-100, 20 mM HEPES, pH 7.5, 150 mM NaCl, 1 mM EDTA, and 0.1% BSA) in the presence of protease inhibitors for 1 h and centrifuged ($1000 \times g$) at 4°C for 30 min. Total lysates (~200 μg of protein) were incubated with 20 μl Protein G PLUS/Protein A-agarose beads (Calbiochem, San Diego, CA) for 1 h, and the supernatant was incubated with 2 μg anti-FLAG (M2) at 4°C for 15 h, followed by 20 μl Protein G PLUS/Protein A agarose beads.

Bound immune complexes were collected in Laemmli sample buffer, separated by 7.5% SDS-PAGE, and immunoblotted with affinity-purified antimegalin (LBD IV) antibody.

Preparation of L2 Cells for Immunofluorescence

L2 cells were fixed in 2% paraformaldehyde (PFA) for 30 min, permeabilized, blocked with 10% fetal calf serum for 10 min, and incubated with primary antibodies for 2 h at 25°C, followed by Alexa Fluor 594-conjugated goat anti-mouse $F(ab')_2$ and/or Alexa 488 goat anti-rabbit $F(ab')_2$, for 1 h. For lysosome detection cells were cultured for 1 h in the presence of LysoTracker Red (Molecular Probes) before fixation. Some L2 cells were incubated in DMEM and treated with 10 μM nocodazole for 1 h before fixation. Images were captured using a Zeiss Axiophot equipped with a Hamamatsu Orca ER charge-coupled device (CCD) camera.

Internalization of Megalin

To follow internalization of megalin, cells were incubated with fresh DMEM without serum for 1 h, cooled on ice, and anti-megalin mAb (20B) (50 μg/ml) was bound to the cells for 15 min at 4°C. Some cells (0-min time point) were rinsed in ice-cold DMEM and fixed with ice-cold 2% PFA for 30 min. The remaining cells were rinsed in ice-cold DMEM, placed in prewarmed DMEM (without serum) at 37°C, and incubated for 2, 5, 10, 15, 30, or 60 min. Cells were then fixed, permeabilized, and incubated with anti-ARH at 25°C as described above. Rabbit IgGs were detected using Alexa 488 goat anti-rabbit $F(ab')_2$, and bound, internalized anti-megalin was visualized using Alexa 594 goat anti-mouse $F(ab')_2$. For semiquantitative analysis of bound and internalized antimegalin IgG, images were calculated as follows. Only pixels with gray scale intensities between 75 and 255 were included and the number of total pixels for anti-megalin on the plasma membrane (PM), those associated with intracellular compartments, and those that overlapped with ARH (yellow pixels) were measured using NIH image (National Institutes of Health, Bethesda, MD); 10–30 cell profiles were measured per time point.

For immunoelectron microscopy cells loaded with anti-megalin antibody for 2 or 60 min were fixed in 2% PFA for 30 min and in 4% PFA for 4 h. Samples were prepared as described previously (Lundstrom *et al*., 1993; Lavoie *et al*., 2002), and ultrathin cryosections were double labeled using anti-ARH for 2 h at 25°C followed by 5-nm gold–conjugated goat anti-rabbit IgG to visualize ARH and 10-nm gold–conjugated goat anti-mouse IgG to visualize internalized megalin.

Binding, Uptake, and Degradation of ^{125}I-Labeled Lactoferrin

Lactoferrin was radiolabeled using Na[^{125}I] and IODO-BEADs (Pierce Chemical, Rockford, IL) (specific activity ~20,000 cpm/ng). Analysis of binding, uptake, and degradation of ^{125}I-labeled human lactoferrin was as described previously (Goldstein *et al*., 1983; Czekay *et al*., 1997). Briefly, 2×10^5 cells were seeded on six-well tissue culture plates and grown for 2 d. Cells were rinsed with media containing 0.1% BSA and incubated with ^{125}I-lactoferrin (5 nM) for 1 or 2 h at 37°C. The medium was removed and adjusted to 15% trichloroacetic acid at 4°C. After 1 h, samples were centrifuged at 15,000 $\times$ *g* at 4°C for 30 min, and the trichloroacetic acid-soluble counts released were quantified by gamma counting, indicating cellular degradation of ^{125}I-labeled lactoferrin. The amount of ^{125}I-labeled lactoferrin degraded was normalized to total cellular protein. Cells were acid washed and the released cell-surface associated radioactivity was quantified by gamma counting (Czekay *et al*., 1997) after which the cells were lysed with 1% SDS and the cell-associated radioactivity quantified.

RESULTS

Identification of ARH as a Megalin Binding Protein

To identify new proteins that interact with the cytoplasmic tail of megalin, we carried out yeast two-hybrid screening of a rat kidney cDNA library by using the region of the megalin cytoplasmic tail that contains the first FXNPXY and the NXXY motif as bait. Among the clones confirmed to be positive, one was found to be a fragment (aa 44–307) of the rat ortholog of human ARH (Garcia *et al*., 2001) that extended from the PTB domain to the C-terminal region. To obtain the complete coding sequence, we carried out 5′ RACE on the same cDNA library. Rat ARH consists of 307 amino acids, is 96.4 and 89.6% identical to mouse and human ARH, respectively, and is one amino acid shorter (Figure 1A). The PTB domain, found in the N-terminal part of ARH (aa 43–174), is conserved among species because it is

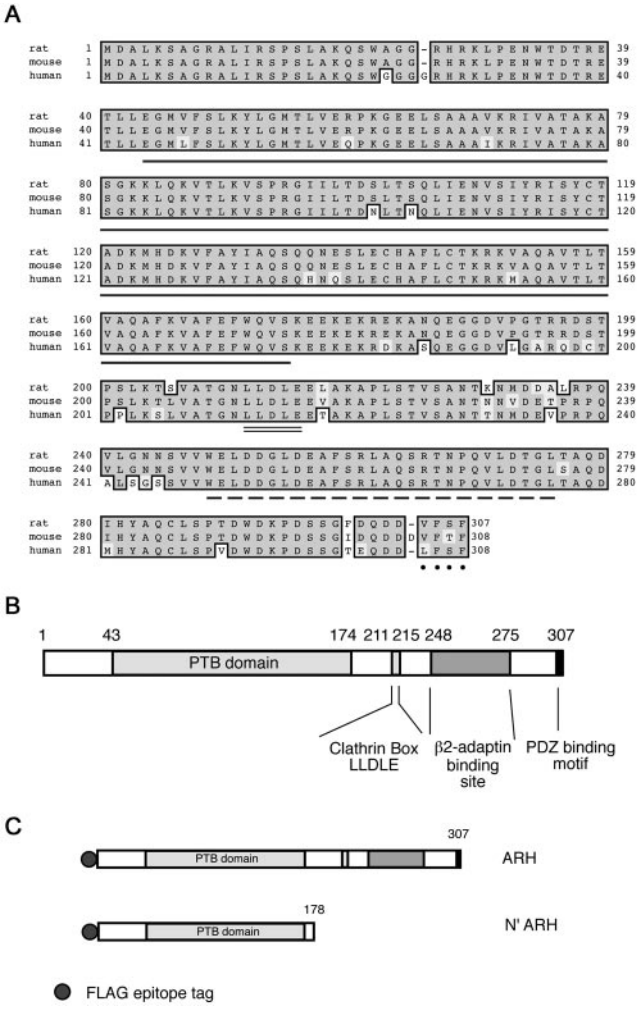

Figure 1. (A) Alignment of the amino acid sequence of rat, mouse, and human ARH. The PTB domain is underlined, the consensus clathrin box is double underlined, the putative AP-2 binding domain is marked with an interrupted underline, and the PDZ binding motif (class II) is dotted. The human and mouse sequences are from Garcia *et al*. (2001). (B) Schematic diagram of the overall domain organization of ARH. (C) Schematic diagrams of full length and N terminal, FLAG-tagged ARH constructs.

100 and 93.9% identical to that of mouse and human ARH. As reported previously for human ARH, rat ARH has a clathrin-box motif (LLDLE), a putative binding site for the β2 subunit of AP-2 (He *et al*., 2002), and a consensus PDZ binding motif (class II) at its C-terminus (-VFSF) (Hung and Sheng, 2002) (Figure 1B).

ARH Interacts with the First FXNPXY Motif of the Cytoplasmic Tail of Megalin

To map the ARH binding site in the cytoplasmic tails of megalin, LRP, and the LDLR, we tested the ability of ARH to interact with each of the FXNPXY motifs of these receptors by two-hybrid, one-to-one interaction assays. We found that ARH interacts with the first FXNPXY motif of megalin but not with the second FXNPXY motif or the NXXY motif. ARH also interacts with the FXNPXY motif of LRP and the LDLR but not with the NPXY motifs of megalin or LRP (Figure 2).

Bait			Prey: rat ARH	Interaction
Megalin	FXNPXY(First)	4490-4511	VGKQPVI**FE**N**P**M**Y**AAKDNKSKV	+
Megalin	NXXY	4523-4544	QVTVPENVE**N**QN**Y**GPPIDPSEI	-
Megalin	FXNPXY(Second)	4569-4590	KPKQTTN**FE**N**P**I**Y**AEMDSEVKD	-
LRP	NPXY	4442-4463	NGAMNVEIG**NP**T**Y**KMYEGGEPD	-
LRP	FXNPXY	4476-4497	DPDKPTN**FT**N**P**V**Y**ATLYMGGHG	+
LDLR	FXNPXY	795-816	KNISNAN**FD**N**P**V**Y**QKTTEDEVH	+

Figure 2. Mapping ARH-binding sites containing the NPXY motifs of megalin, LRP, and LDLR by using the yeast two-hybrid system. The FXNPXY motifs are shown in bold. Results of interaction between bait and prey are shown by (+) or (−). Bait and prey constructs were cotransformed into yeast strain EGY48 with the reporter vector. Transformants were plated onto selective medium, and colonies that survived were exposed to standard UV light.

Megalin Tail Interacts with ARH in Pull-Down and Immunoprecipitation Assays

We also performed in vitro GST pull-down assays and found that in vitro-translated ARH bound strongly to GST-MT but not to GST alone (Figure 3A).

To demonstrate interaction of megalin with ARH in vivo, we prepared MDCK-M4-ARH cells stably expressing megalin mini-receptor (M4) (Figure 4) and FLAG-tagged, full-length ARH (Figure 1C) and carried out immunoprecipitation with anti-FLAG (M2) followed by immunoblotting for megalin. We found that megalin mini-receptor coimmunoprecipitated with full-length ARH (Figure 3B). This result indicates that the megalin specifically interacts with ARH in vivo.

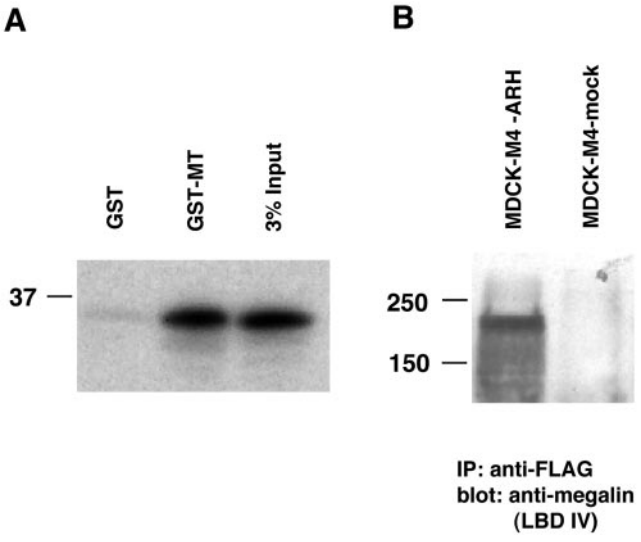

Figure 3. (A) Interaction of GST-megalin tail with ARH in a GST pull-down assay. ARH binds specifically to GST megalin tail but not to GST alone. GST-MT and GST alone (~5 mg) bound to glutathione-agarose beads were incubated with in vitro translated, radiolabeled rat ARH. The precipitates were separated by 12.5% SDS-PAGE and detected by autoradiography. 3% Input-3% of the in vitro-translated products. (B) Megalin mini-receptor 4 (M4) coimmunoprecipitates with ARH. MDCK-M4-ARH cells (which express megalin mini-receptor and FLAG-tagged ARH) and MDCK-M4-mock cells (which express megalin mini-receptor but not ARH) were lysed, immunoprecipitated with anti-FLAG (M2), and the precipitated proteins were separated by 7.5% SDS-PAGE and immunoblotted with anti-megalin (LBD IV) anti-serum (1:2000).

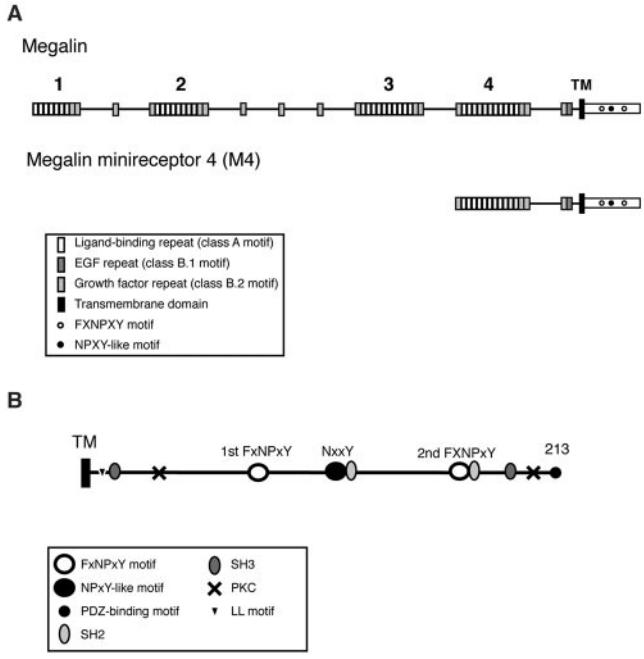

Figure 4. Schematic representation of megalin and megalin mini-receptor (A) and the cytoplasmic tail of megalin (B). Megalin contains four ligand binding domains, LBD 1–4. Megalin mini-receptor 4 (M4) includes LBD 4, the transmembrane (TM) domain, and the cytoplasmic tail (CT) of megalin. The megalin cytoplasmic tail contains a number of potential sorting and endocytosis motifs, including FXNPXY, NXXY, di-leucine, SH2, SH3, protein kinase C (PKC), and PDZ binding motifs.

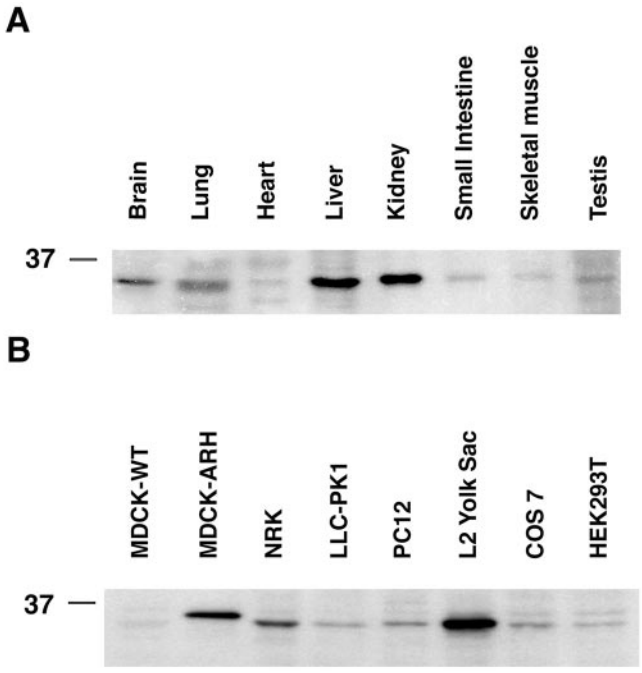

Figure 5. Expression and distribution of ARH in tissues and cell lines. (A) ARH expression is highest in kidney and liver, less in brain, and lung and lower in heart, small intestine, skeletal muscle, and testis. (B) ARH is highly expressed in L2 cells, MDCK-M4-ARH, and NRK cells. Expression of ARH in LLC-PK1, PC12, COS 7, and HEK293T cells is much lower. ARH is expressed in trace amounts in wild-type MDCK cells (MDCK-WT). Twenty micrograms (cells) or 30 μg (rat tissues) of total protein were separated by 12.5% SDS-PAGE, transferred to polyvinylidene difluoride membranes, and probed with affinity-purified anti-ARH.

ARH Is Highly Expressed in Rat Brain, Lung, Heart Liver, Kidney, and Testis

We next examined the tissue distribution of ARH in organ lysates by immunoblotting. ARH was detected in all tissues examined, but expression was highest in liver, kidney, brain, and lung, and lower in heart, small intestine, skeletal muscle, and testis (Figure 5A). With the exception of the liver, the organs with highest levels of expression of ARH coincide with those expressing the highest levels of megalin (Zheng *et al*., 1994). LRP and the LDL receptor are known to be highly expressed in the liver.

ARH Is Highly Expressed in Normal Rat Kidney (NRK) Cells and L2 Cells

We also checked for the presence of ARH in a number of cell lines and found that ARH was widely expressed. It was most abundant in L2 cells and NRK cells and less abundant in LLC-PK1, PC12, COS 7, and HEK293T cells. Interestingly, expression of endogenous ARH in L2 cells was greater than in MDCK-M4-ARH cells stably overexpressing FLAG-tagged ARH (Figure 5B). L2 cells also express the highest level of endogenous megalin of any cell line we have analyzed (Lou *et al*., 2002). Thus, L2 cells provide an excellent model for investigating the interaction between ARH and megalin.

ARH Colocalizes with Megalin and Several Endocytic Markers in L2 Cells

Next, we carried out double labeling of L2 cells by immunofluorescence by using affinity-purified anti-ARH and anti-megalin mAb 20B IgG. Megalin is known to be distributed in CCPs and the endosomal system in these cells (Lundstrom *et al*., 1993; Czekay *et al*., 1997). At steady state, ARH was concentrated along the plasma membrane and was also found inside the cell in a juxtanuclear spot where it overlapped with megalin (Figure 6, A–C). Similar findings were obtained on LLC-PK1 cells (our unpublished data), which also express megalin (Lou *et al*., 2002). To more precisely define the compartments where ARH is found, we carried out double labeling for ARH and endocytic markers in L2 cells. ARH partially colocalized with AP-2 in CCPs along the plasma membrane (Figure 6, D–F) and with the early endosome marker EEA1 (Figure 6, G–I). ARH also colocalized with the recycling endosome marker Rab11 (Ullrich *et al*., 1996) (Figure 6, J–I) and with the transferrin receptor (TFR) (Figure 6, M–O) in the juxtanuclear Golgi region where both are known to be associated with recycling endosomes. Staining for ARH did not overlap appreciably with LysoTracker, a marker for lysosomes (Figure 6, P–R). These findings indicate ARH is associated with the plasma membrane, early endosomes, and recycling endosomes but not with lysosomes in L2 cells.

ARH and Megalin Internalization and Recycling

We next examined the fate of megalin and ARH in L2 cells after tagging megalin with a mAb that binds to the ectodomain of the receptor. L2 cells were incubated with DMEM without serum for 1 h (allows accumulation of megalin at the cell surface), mAb 20B was bound to the cell surface at 4°C, after which the cells were warmed to 37°C to allow the antibody-tagged megalin to enter the cell. After binding at 4°C, megalin and ARH colocalized along the plasma membrane of L2 cells (Figure 7, A–C). After 2 min at 37°C (Figure 7, D–F), some of the megalin and ARH were found inside the cell where they colocalized, whereas some megalin and ARH remained at the cell surface. After 5 (Figure 7, G–I), 10 and 15 min, most of the megalin and ARH colocalized inside the cell in the juxtanuclear region. Beginning at 30 min (Figure 7, J–L) and especially at 60 min (Figure 7, M–O) some of the megalin had returned to the plasma membrane where it colocalized with ARH. Semiquantitative analysis (Figure 7, P–R) showed megalin is rapidly and efficiently internalized, as it was already seen inside the cell by 2 min. By 5 min, 50% and by 15 min most (87%) of the megalin had been internalized. By 15 min, the tagged megalin had already started to return to the PM with >50% having reappeared by 60 min (Figure 7, Q and R). During the internalization and recycling process the overlap with ARH showed the exact same trend: colocalization with megalin at the PM was highest at 0 min and gradually declined from 2 to 15 min and rose again at 60 min (Figure 7R). Collectively, these experiments suggest that megalin and ARH are internalized together on CCPs and travel to early endosomes and then to the Golgi region where they overlap with markers for recycling endosomes, after which they return to the PM.

Juxtanuclear ARH Disperses after Nocodazole Treatment

To verify that intracellular ARH is concentrated in recycling endosomes, we treated L2 cells and NRK cells with nocodazole, a microtubule-depolymerizing agent. It has been shown that nocodazole treatment causes recycling endo-

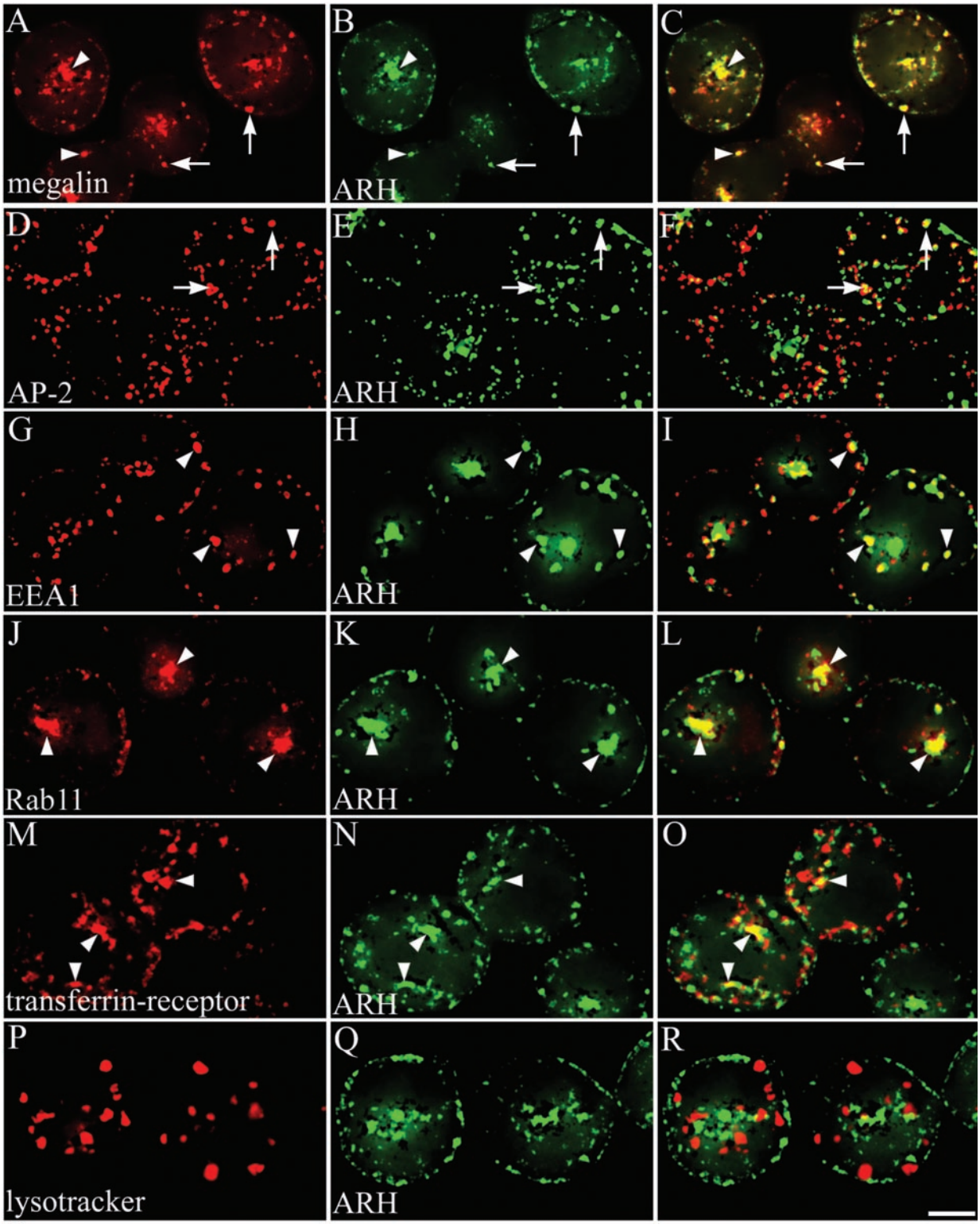

Figure 6. Immunofluorescence localization of ARH, megalin, and endocytic markers in L2 cells. Fixed and permeabilized L2 cells were incubated with affinity-purified anti-ARH IgG (B, E, H, K, N, and Q) and either anti-megalin 20B (A), anti-AP-2 (D), anti-EEA1 (G), anti-Rab11 (J), anti-TFR (M), or LysoTracker Red (P), followed by goat anti-rabbit Alexa 488 and anti-mouse Alexa 594 $F(ab')_2$. ARH and megalin are concentrated at the cell periphery (arrowheads) and in the juxtanuclear region. The distribution of ARH partially overlaps with AP-2, EEA1, Rab11, and TFR but not with LysoTracker. Arrows indicate overlap at the PM, arrowheads indicate intracellular colocalization. Bar, 2 μm.

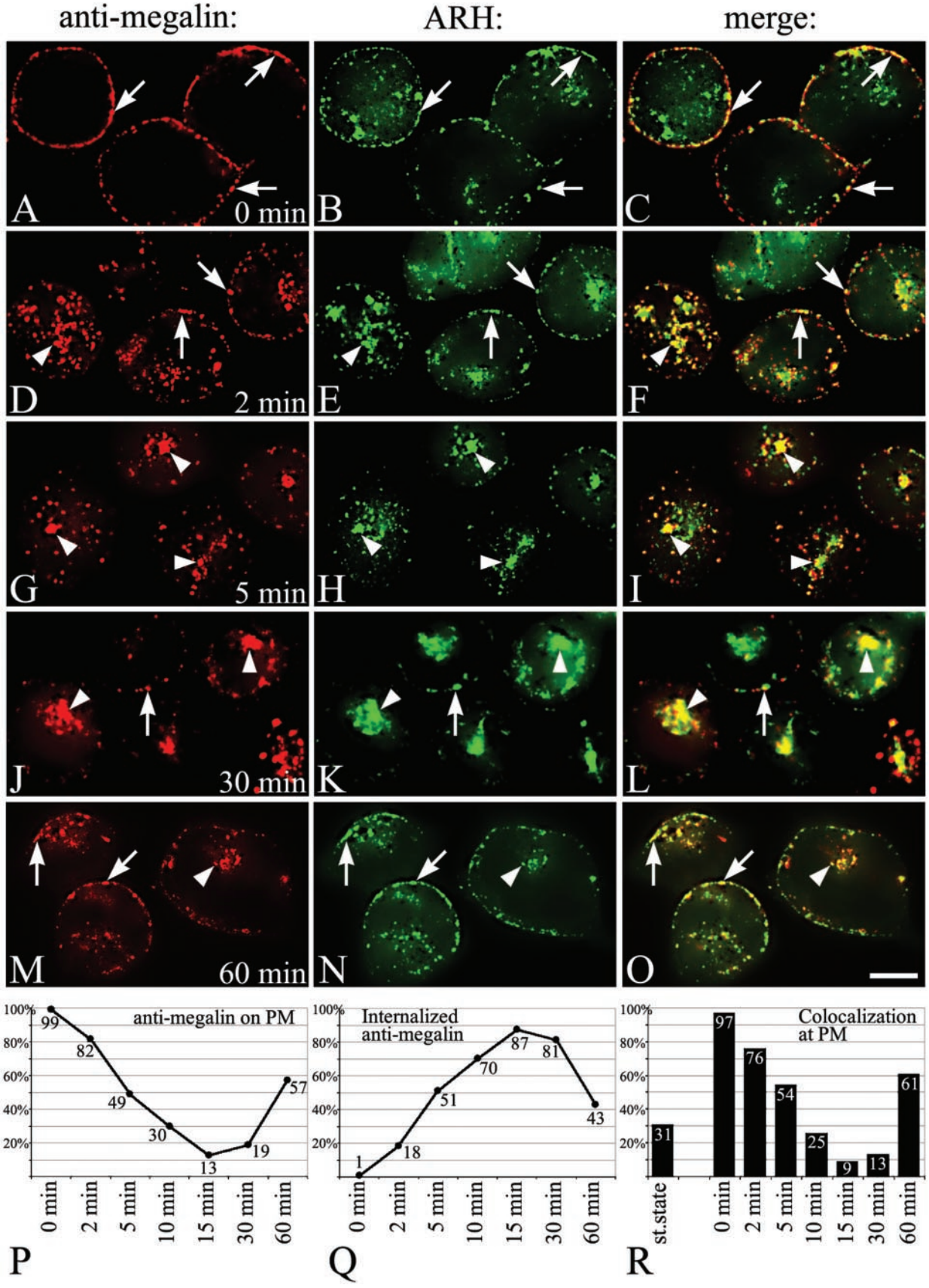
anti-megalin:
ARH:
merge:
A
0 min
B
C
D
2 min
E
F
G
5 min
H
I
J
30 min
K
L
M
60 min
N
O
anti-megalin on PM
99
82
49
30
13
19
57
100%
80%
60%
40%
20%
0 min
2 min
5 min
10 min
15 min
30 min
60 min
P
Internalized anti-megalin
1
18
51
70
87
81
43
Q
Colocalization at PM
31
97
76
54
25
9
13
61
st.state
R

Figure 7.

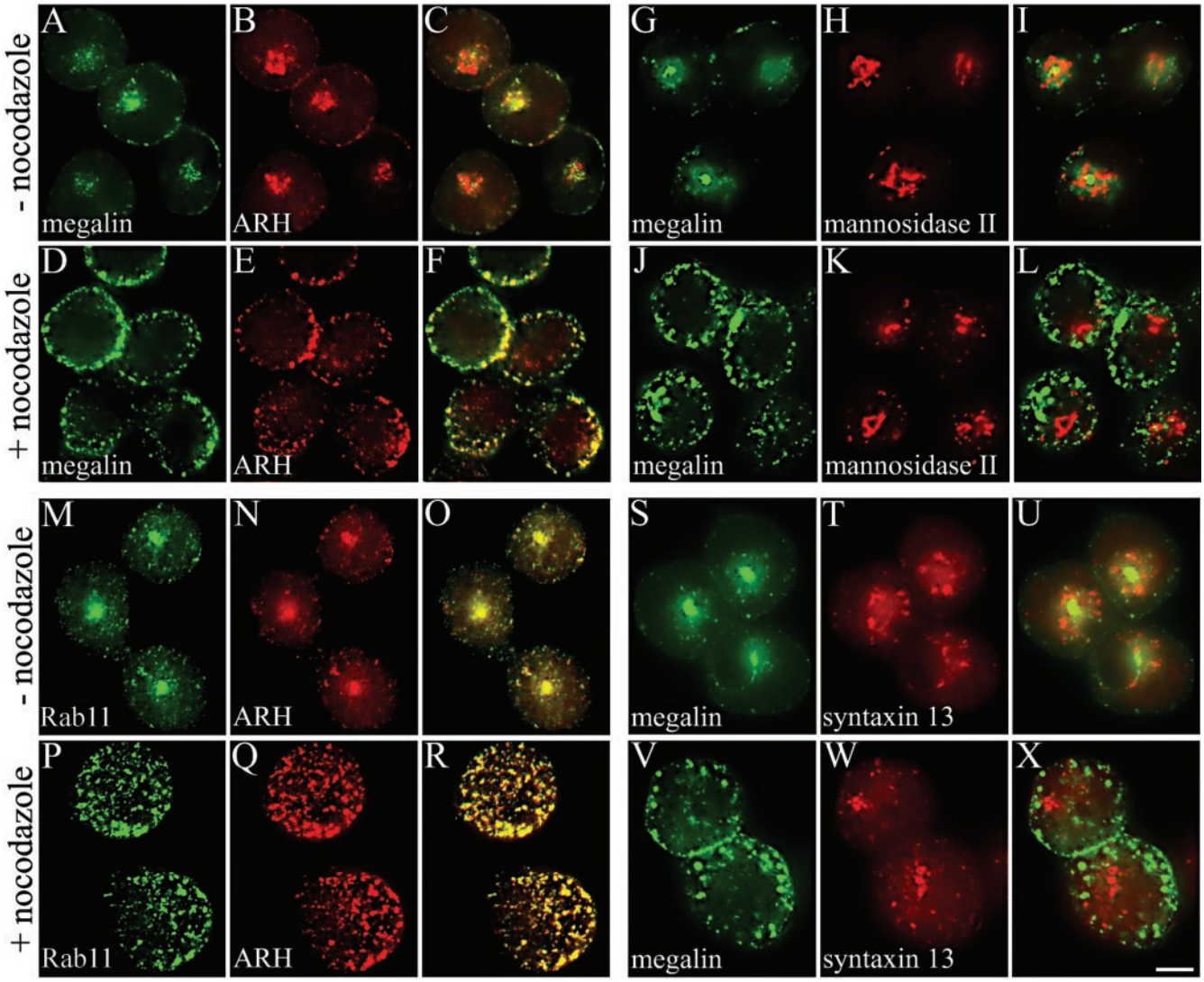

Figure 8. Nocodazole disperses juxtanuclear ARH staining. L2 cells were incubated in the presence (+) or absence (−) of 10 μM nocodazole, fixed with 2% paraformaldehyde, permeabilized, and incubated with anti-megalin mAb 20B (A, D, G, J, S, and V), anti-ARH (B, E, N, and Q), anti-α-mannosidase II (H and K), anti-rab11 (M and P), or anti-syntaxin 13 (T and W) followed by goat anti-mouse Alexa 488 and anti-rabbit Alexa 594 F(ab')$_2$. Treatment of L2 cells with nocodazole caused dispersal of the ARH and megalin positive juxtanuclear compartment into multiple vesicular structures scattered throughout the cytoplasm (A–F), whereas the Golgi marker α-mannosidase II did not disperse (G–L). Staining for ARH overlaps with the recycling endosome marker Rab11 before and after treatment with nocodazole (M–R). Staining for syntaxin 13 overlaps with megalin in untreated cells but does not disperse after nocodazole treatment (S–X). Bar, 2 μm.

Figure 7 (facing page). Megalin internalization. L2 cells precultured (1 h) in serum-free media were incubated with mouse anti-megalin mAb 20B on ice for 15 min, warmed to 37°C for 0 (A–C), 2 (D–F), 5 (G–I), 30 (J–L), or 60 min (M–O), fixed, and incubated with anti-ARH followed by goat anti-rabbit Alexa 488 (to detect ARH) and anti-mouse Alexa 594 F(ab')$_2$ (to detect megalin). After binding at 4°C, megalin and ARH colocalize along the plasma membrane (arrows) of L2 cells. After 2 min at 37°C, some of the megalin is found inside the cell (arrowheads) with some still remaining at the cell surface. At 5 or 30 min, most of the megalin and ARH colocalize inside the cell. After 60 min, some of the megalin returns to the plasma membrane (arrows) where it colocalizes with ARH. Arrows indicate overlap at the PM, arrowheads indicate intracellular colocalization. Bar, 2 μm. (P–R) Semiquantitative analysis of bound and internalized anti-megalin. Images were thresholded as described under MATERIALS AND METHODS, and positive pixel areas for anti-megalin on the PM (P), internalized anti-megalin (Q), and antimegalin pixels that were also positive for ARH (yellow pixels) (R) were measured.

somes (but not Golgi cisternae) in the pericentriolar region to disperse into multiple vesicular structures scattered throughout the cytoplasm (Matteoni and Kreis, 1987; Prekeris *et al*., 1998; Mammoto *et al*., 1999). Treatment of L2 cells with nocodazole scattered the ARH-positive juxtanuclear compartment with megalin to the cell periphery in both L2 cells (Figure 8, A–F) and NRK cells (our unpublished data), but the Golgi marker, α-mannosidase II was unaffected (Figure 8, J–L). We next examined the behavior of Rab11 and syntaxin 13 after nocodozole treatment of L2 cells. Rab11 (Ullrich *et al*., 1996; Sonnichsen *et al*., 2000) and syntaxin 13 (Prekeris *et al*., 1998; Trischler *et al*., 1999; Collins *et al*., 2002) are reported to be markers for recycling endosomes. We found that in L2 cells Rab11 dispersed upon nocodazole treatment and colocalized with ARH and megalin both be-

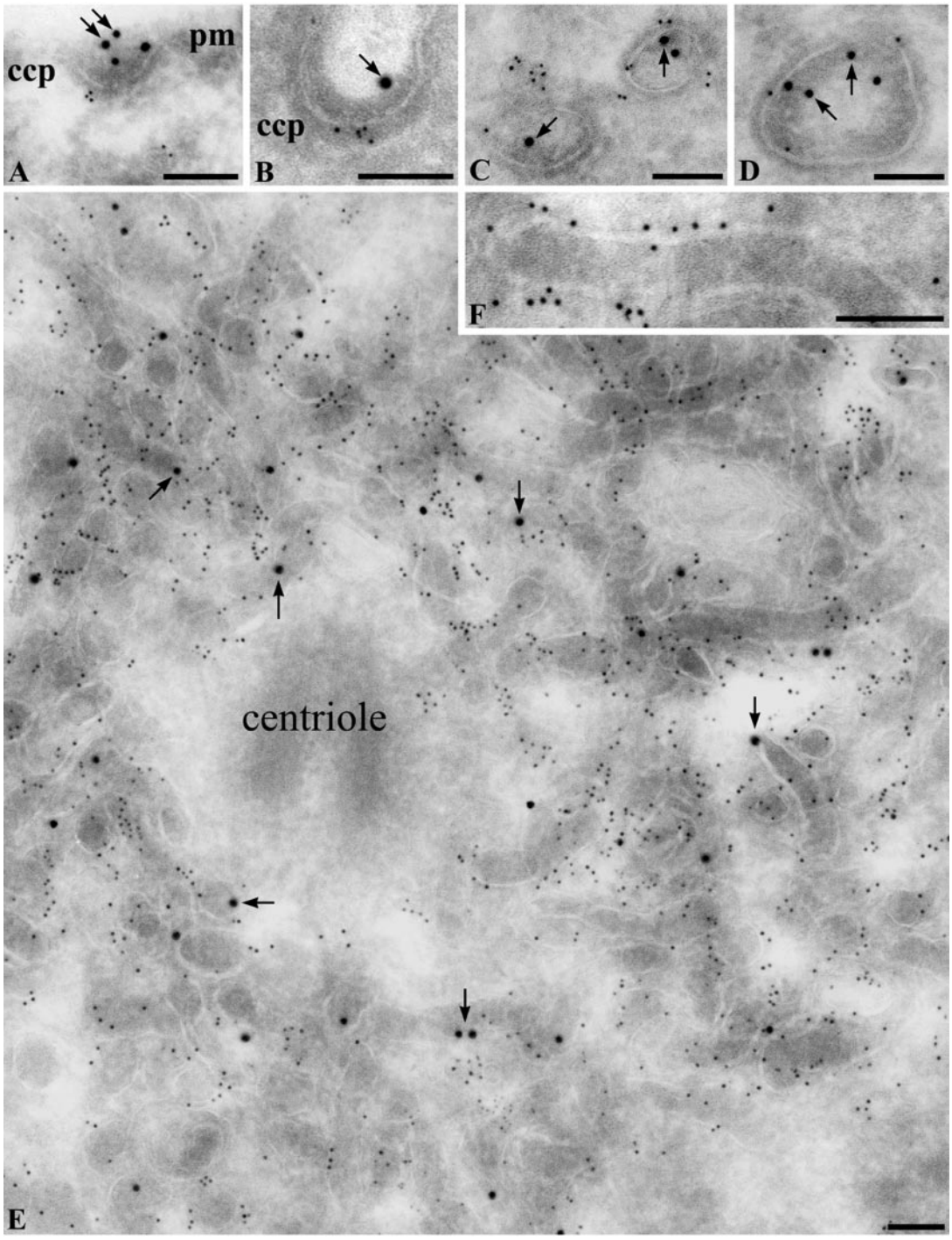

Figure 9. Immunogold localization of ARH and megalin in L2 cells. Cells were allowed to take up anti-megalin IgG for 2 min or 60 min at 37°C before fixation and then incubated with affinity-purified anti-ARH IgG after fixation followed by incubation with 5-nm gold conjugated goat anti-rabbit or 10 nm anti-mouse IgG conjugates as described under MATERIALS AND METHODS. (A–D) Cells loaded with anti-megalin mAb 20B IgG for 2 min before fixation. Megalin (arrows, 10-nm gold) and ARH (5-nm gold) colocalize at clathrin coated pits (A and B) located along the PM. Some ARH (small gold) is associated with vesicles (C) or endosomes (D) located near the cell membrane. (E and F) Cells loaded with anti-megalin mAb 20B IgG for 60 min before fixation. Megalin (arrows, 10-nm gold) and ARH (5-nm gold) are found on abundant networks of dense tubules concentrated in the pericentriolar region that correspond in morphology to recycling endosomes. ccp, clathrin coated pit. pm, plasma membrane. Arrows indicate megalin (large gold). Bars, 100 nm.

fore and after treatment (Figure 8, M–R), whereas syntaxin 13 staining overlapped with megalin in untreated cells but did not disperse and did not colocalize with megalin after nocodazole treatment (Figure 8, S–X). We conclude that the fate of Rab11 and syntaxin 13 after nocodazole treatment differs: ARH is mainly localized to recycling endosomes that

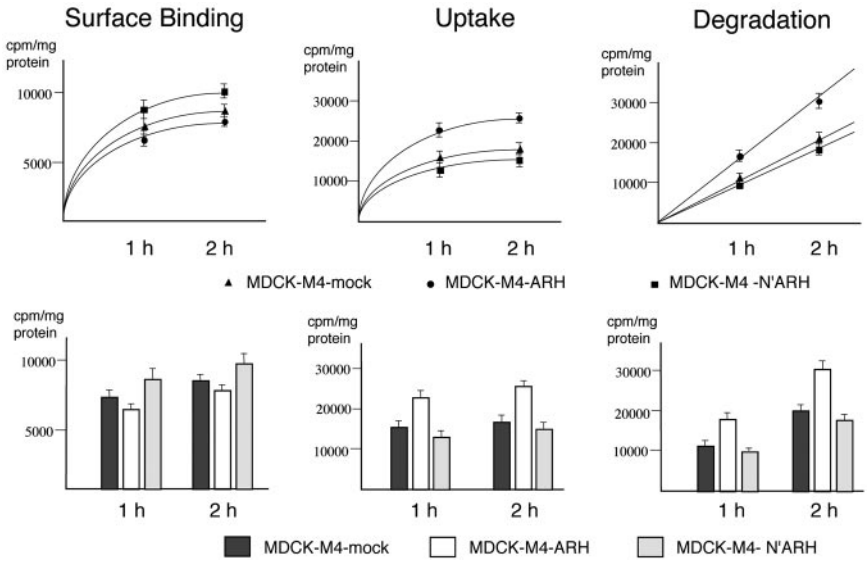

Figure 10. Effect of ARH on megalin mediated uptake and degradation of ^{125}I-lactoferrin. MDCK-M4-ARH cells (2×10^5) stably expressing full-length ARH, the N terminus of ARH (MDCK-M4-N′ARH) or mock-transfected cells (MDCK-M4 mock), were seeded on six-well tissue culture plates and grown for 2 d before the experiments. Cells were rinsed (three times) with media containing 0.1% BSA and incubated with 5 nM ^{125}I-lactoferrin for 1 or 2 h at 37°C in the presence or absence of unlabeled ligand (100 nM). Binding, uptake, and degradation of ^{125}I-lactoferrin were determined as described under MATERIALS AND METHODS. Upper panels: Surface binding of labeled lactoferrin is similar or slightly decreased in MDCK-M4-ARH cells, but uptake and degradation of lactoferrin in cells expressing full-length ARH are significantly increased. By contrast, in cells expressing N′ARH, uptake and degradation are unchanged or slightly decreased. Lower panels: Graphs of data shown in upper panels. Data are presented as means ± SD of three independent experiments.

are associated with Rab11, whereas syntaxin 13 marks a different subdomain of recycling endosomes than Rab11.

ARH Colocalizes with Megalin at Clathrin Coated Pits and Juxtanuclear Tubulovesicular Structures after Immunogold Labeling

To confirm and extend the results obtained by immunofluorescence, we carried out immunogold labeling for megalin and ARH on ultrathin cryosections of L2 cells after tagging megalin with mAb 20B IgG as described above. After 2 min at 37°C, ARH colocalized with megalin at CCPs and vesicles along the plasma membrane (Figure 9, A–C) and in endosomes located near the plasma membrane (Figure 9D). After 60 min, ARH and megalin colocalized in abundant dense tubular structures located in the juxtanuclear region that correspond in morphology to recycling endosomes (Figure 9, E and F) (Hopkins and Trowbridge, 1983). The tubular structures with megalin and ARH were typically concentrated around the centrioles in the pericentriolar, microtubule organizing center and possessed dense contents as is characteristic for recycling endosomes. These data reinforce the immunofluorescence results by showing the precise localization of ARH and megalin in tubular structures corresponding in morphology to recycling endosomes.

ARH Facilitates Uptake and Degradation of ^{125}I-Lactoferrin by Megalin

To examine the effect of ARH on megalin-mediated endocytosis, we carried out an endocytosis assay by using ^{125}I-labeled lactoferrin as ligand (Figure 10) on confluent MDCK-M4 cells, which stably express megalin mini-receptors and either full-length ARH or truncated, N′ARH, a mutant containing the PTB domain but lacking the C terminus. This mutant would be expected to bind to megalin but not to clathrin or AP-2 (Figure 1C). We chose MDCK cells for expression of ARH because they express little or no endogenous ARH (Figure 5B) and because uptake assays can be done from the apical surface without competition from LDLR and LRP, which are expressed on the basolateral domain of MDCK cells (Takeda *et al*., 2003). Both wild-type ARH and the ARH truncation mutant are concentrated in the juxtanuclear region, and expression of either full-length or the mutant ARH did not affect the distribution of either megalin or LRP as assessed by confocal microscopy and cell surface biotinylation. LRP also binds lactoferrin, but LRP is expressed exclusively on the basolateral surfaces of MDCK cells, which are not exposed when MDCK cells reach confluence. When binding, uptake, and degradation of ^{125}I-labeled lactoferrin by MDCK-M4-ARH, MDCK-M4-N′ARH, and MDCK-M4-mock cells were compared, we found that surface binding of labeled lactoferrin was similar or slightly decreased, but uptake and degradation of lactoferrin in cells expressing ARH were significantly increased (58 and 51%, respectively). These results indicate that overexpression of ARH facilitates megalin-mediated endocytosis and degradation of ligand. In the presence of N′ARH (which lacks the C-terminus), uptake and degradation were unchanged or slightly decreased.

DISCUSSION

Sorting of proteins during endocytosis depends on the interaction between sorting signals present in the cytosolic domains of various receptors and adaptor proteins that are components of protein coats (Bonifacino and Traub, 2003). The oldest sorting signal is the FXNPXY motif originally found >15 years ago in the LDLR (Davis *et al*., 1986; Chen *et al*., 1990). Three adaptor proteins have been shown to interact with FXNPNY motifs of the LDLR-- AP-2, Dab 2, and ARH (Morris and Cooper, 2001; Boll *et al*., 2002; He *et al*., 2002; Mishra *et al*., 2002a,b). We report here that ARH also binds to the first FXNPXY signal of megalin, presumably in CCPs, and facilitates megalin's transport along the recycling endocytic pathway. When megalin's trafficking was followed by tagging it with a nonperturbing mAb, ARH colocalized with megalin throughout its entire intracellular journey from coated pits to early endosomes to recycling endosomes and back to the cell surface. That ARH facilitates megalin's transport through the endosomal system is indicated by our finding that in MDCK cells expressing both ARH and megalin, uptake and degradation of ^{125}I-lactoferrin, a megalin ligand, is enhanced.

The C terminus of ARH has been shown to interact with the N terminus of clathrin through its clathrin box sequence

(LLDLE) and with the β2-adaptin subunit of AP-2 through its C-terminal region in vitro (He *et al*., 2002; Mishra *et al*., 2002b) as well as to the FXNPXY sequences of LDLR, megalin, and LRP. Thus, ARH serves to couple megalin to the endocytic machinery. Several other proteins, i.e., β-arrestin and clathrin heavy chain, also bind to the β2 subunit of AP-2, whereas Dab2 binds to the α subunit and YXXØ motifs to the μ2 subunit of AP-2 (Morris and Cooper, 2001; Kirchhausen, 2002). Our finding that the N′ARH mutant, which lacks the clathrin and AP-2 binding domains as well as the PDZ binding motif, fails to facilitate megalin endocytosis indicates that binding of ARH to the FXNPXY motif is not sufficient to stimulate uptake, and additional interactions of the C terminus of ARH are required. ARH has a class II PDZ binding motif at its C terminus, which suggests that in addition to clathrin and AP-2, it can bind to one or more PDZ proteins. PDZ proteins function as scaffold proteins that typically serve to cluster signaling complexes and membrane proteins (Nourry *et al*., 2003). Thus, a key element in understanding the functions of ARH in megalin trafficking and signaling is to identify the PDZ protein(s) that bind to ARH.

We found that at steady state a large fraction of the ARH is associated with recycling endosomes in the juxtanuclear (Golgi) region in L2 cells and in several other cell types, including LLC-PK1 cells, that express megalin; NRK cells, which express LRP but not megalin; and MDCK cells stably expressing megalin mini-receptors and ARH. We also found that in kidney proximal tubules where megalin is abundantly expressed (Kerjaschki *et al*., 1984), ARH is concentrated in characteristic "dense apical tubules" (Nagai *et al*., 2003), which correspond to recycling endosomes (Christensen and Birn, 2002). Mishra *et al*. (2002b) previously localized ARH mainly to CCPs by immunofluorescence but also reported that ARH, in contrast to Dab2, was not concentrated in brain or liver coated vesicle fractions, which is in keeping with our observation that much of the ARH is present in recycling endosomes. Based on their finding that separation of ARH and LDLR occurred 2 min after ligand uptake in HeLa cells, these authors suggested that ARH acts at the cell surface and does not progress with cargo into budded vesicles and instead may hand off LDLR to Dab2. Our results are more compatible with a model according to which megalin binds first to AP-2 and/or Dab2 in CCPs, and Dab2 hands-off megalin to ARH, which escorts megalin to and through early endosomes and recycling endosomes. The differences between our results and those of Mishra and coworkers may lie in different receptors, cell lines, or experimental conditions. One key difference between LDLR and megalin is that megalin has two FXNXPY signals, whereas LDLR and its other family members have only one.

The fact that ARH seems to accompany megalin to and through endosomes raises the question of whether transport of megalin through the endosomal system occurs by bulk flow as usually assumed or whether it is selective and requires specific adaptor proteins. The findings that patients with hypercholesterolemia due to mutations in ARH fail to take up LDL and that retroviral expression of normal ARH restores LDLR internalization (Eden *et al*., 2002) together with our findings suggest that ARH is essential for transport of some LDLR family members through the endosomal system in some cell types.

The cytoplasmic tail of megalin contains two FXNPXY motifs and one similar NXXY motif (Figure 4). Our recent studies using deletion mutants of the megalin tail revealed that both FXNPXY motifs play a role in endocytosis of megalin, whereas the region encompassing the NXXY motif lacking phenylalanine directs the apical sorting of megalin (Takeda *et al*., 2003). Our mapping studies demonstrated that ARH interacts with the first FXNPXY motif but not with the NXXY and second FXNPXY motif. This is in contrast to Dab 2 which interacts preferably with the second FXNPXY motif (Oleinikov *et al*., 2000). We also showed that ARH interacts with the FXNPXY motif of LRP but not with the NPXY motif, suggesting that ARH could also bind to LRP and affect its trafficking. The phenylalanine residue at two positions amino-terminal to the asparagine seem to be required for interaction of both megalin and LRP with ARH. The phenylalanine residue in the same position is known to be required for optimal internalization of LDLR (Chen *et al*., 1990).

Both Dab2 and ARH have the ability to interact with AP-2, clathrin, and phosphoinositides as well as FXNPXY motifs (Morris and Cooper, 2001; He *et al*., 2002; Mishra *et al*., 2002a,b). Moreover, the PTB domain of ARH is the closest relatively of Dab2 among PTB domains. This raises the possibility that ARH and Dab2 could compensate for one another in endocytosis, which is in keeping with the fact that, in contrast to hepatocytes, defects in LDLR function are not found in cultured fibroblasts from ARH patients. Fibroblasts, but not hepatocytes, express Dab2 at high levels (Garcia *et al*., 2001; Mishra *et al*., 2002b). The fact that Dab2 is highly expressed in the kidney proximal tubule (Oleinikov *et al*., 2000; Morris *et al*., 2002) may also explain why symptoms of megalin deficiency in kidney function, particularly proteinuria, have not been reported in patients with autosomal recessive hypercholesterolemia, whereas megalin knockout mice have severe impairment of kidney function as well as deficiencies in brain development (Willnow *et al*., 1996; Nykjaer *et al*., 1999). Reciprocally, ARH may also compensate for Dab2, as Dab2 knockout mice have only a mild phenotype compared with megalin knockout mice (Morris *et al*., 2002); they are outwardly normal and do not exhibit defective forebrain development or severe kidney malfunction.

Evidence that the juxtanuclear compartment with which ARH is associated corresponds to recycling endosomes was obtained using nocodazole and by its colocalization with Rab11. Juxtanuclear recycling endosomes are maintained by microtubules (Yamashiro *et al*., 1984), and depolymerization of microtubules causes the dispersion of recycling endosomes but not of Golgi cisternae (Prekeris *et al*., 1998). The intracellular compartment where ARH and megalin codistribute was dispersed by treatment of nocodazole, but the Golgi marker α-mannosidase II was not, providing further evidence that ARH is concentrated in recycling endosomes. Both Rab11, a small GTPase (Ullrich *et al*., 1996; Sonnichsen *et al*., 2000), and syntaxin 13, a t-snare (Prekeris *et al*., 1998), are thought to be markers for recycling endosomes. Definitive localization of ARH was obtained by immunoelectron microscopy. ARH was seen to be associated predominantly with a pericentriolar, electron-dense tubular network characteristic of recycling endosomes (Hopkins *et al*., 1994; Gruenberg and Maxfield, 1995; Sachse *et al*., 2002). Preliminary immunoelectron microscopic studies show that syntaxin 13 is localized to tubulovesicular structures in L2 cells that are morphologically distinct from ARH-containing tubules. Our immunofluorescence results show that the distribution of syntaxin 13 and Rab11 are very different in L2 cells, because Rab11 but not syntaxin 13 dispersed after nocodazole treatment. Thus, these markers seem to be present in different subcompartments of recycling endosomes, and ARH and Rab11 share the same subcompartment. This may be a cell-

specific phenomenon as syntaxin 13 disperses after nocodazole treatment of NRK cells (Prekeris *et al*., 1998).

In summary, in this report we demonstrate that ARH is a new partner of the first FXNPXY motif of megalin, and ARH and megalin codistribute in the endosomal system. We further show that ARH facilitates megalin's endocytic trafficking and demonstrate ARH is a new marker for recycling endosomes. Further studies will be required to define the functional interactions of ARH with other trafficking and signaling molecules to unravel the precise role of ARH in endocytosis and recycling of megalin and other members of the LDLR gene family.

ACKNOWLEDGMENTS

This research was supported by National Institutes of Health grant DK17724 (to M.G.F.).

REFERENCES

Altschul, S.F., Gish, W., Miller, W., Myers, E.W., and Lipman, D.J. (1990). Basic local alignment search tool. J. Mol. Biol. *215*, 403–410.

Boll, W., Rapoport, I., Brunner, C., Modis, Y., Prehn, S., and Kirchhausen, T. (2002). The m2 subunit of the clathrin adaptor AP-2 binds to FDNPVY and YppO sorting signals at distinct sites. Traffic *3*, 590–600.

Bonifacino, J.S., and Traub, L.M. (2003). Signals for sorting of transmembrane proteins to endosomes and lysosomes. Annu. Rev. Biochem. *72*, 395–447.

Chatelet, F., Brianti, E., Ronco, P., Roland, J., and Verroust, P. (1986). Ultrastructural localization by monoclonal antibodies of brush border antigens expressed by glomeruli. I. Renal distribution. Am. J. Pathol. *122*, 500–511.

Chen, W.J., Goldstein, J.L., and Brown, M.S. (1990). NPXY, a sequence often found in cytoplasmic tails, is required for coated pit-mediated internalization of the low density lipoprotein receptor. J. Biol. Chem. *265*, 3116–3123.

Christensen, E.I., and Birn, H. (2002). Megalin and cubilin: multifunctional endocytic receptors. Nat. Rev. Mol. Cell. Biol. *3*, 256–266.

Christensen, E.I., Birn, H., Verroust, P., and Moestrup, S.K. (1998). Membrane receptors for endocytosis in the renal proximal tubule. Int. Rev. Cytol. *180*, 237–284.

Christensen, E.I., and Willnow, T.E. (1999). Essential role of megalin in renal proximal tubule for vitamin homeostasis. J. Am. Soc. Nephrol. *10*, 2224–2236.

Collins, R.F., Schreiber, A.D., Grinstein, S., and Trimble, W.S. (2002). Syntaxins 13 and 7 function at distinct steps during phagocytosis. J. Immunol. *169*, 3250–3256.

Czekay, R.P., Orlando, R.A., Woodward, L., Lundstrom, M., and Farquhar, M.G. (1997). Endocytic trafficking of megalin/RAP complexes: dissociation of the complexes in late endosomes. Mol. Biol. Cell *8*, 517–532.

Davis, C.G., Lehrman, M.A., Russell, D.W., Anderson, R.G., Brown, M.S., and Goldstein, J.L. (1986). The J. D. mutation in familial hypercholesterolemia: amino acid substitution in cytoplasmic domain impedes internalization of LDL receptors. Cell *45*, 15–24.

Eden, E.R., Patel, D.D., Sun, X.M., Burden, J.J., Themis, M., Edwards, M., Lee, P., Neuwirth, C., Naoumova, R.P., and Soutar, A.K. (2002). Restoration of LDL receptor function in cells from patients with autosomal recessive hypercholesterolemia by retroviral expression of ARH1. J. Clin. Investig. *110*, 1695–1702.

Farquhar, M.G., Saito, A., Kerjaschki, D., and Orlando, R.A. (1995). The Heymann nephritis antigenic complex: megalin (gp330) and RAP. J. Am. Soc. Nephrol. *6*, 35–47.

Finer, M.H., Dull, T.J., Qin, L., Farson, D., and Roberts, M.R. (1994). kat: a high-efficiency retroviral transduction system for primary human T lymphocytes. Blood *83*, 43–50.

Garcia, C.K., *et al*. (2001). Autosomal recessive hypercholesterolemia caused by mutations in a putative LDL receptor adaptor protein. Science *292*, 1394–1398.

Goldstein, J.L., Basu, S.K., and Brown, M.S. (1983). Receptor-mediated endocytosis of low-density lipoprotein in cultured cells. Methods Enzymol. *98*, 241–260.

Gotthardt, M., Trommsdorff, M., Nevitt, M.F., Shelton, J., Richardson, J.A., Stockinger, W., Nimpf, J., and Herz, J. (2000). Interactions of the low density lipoprotein receptor gene family with cytosolic adaptor and scaffold proteins suggest diverse biological functions in cellular communication and signal transduction. J. Biol. Chem. *275*, 25616–25624.

Gruenberg, J., and Maxfield, F.R. (1995). Membrane transport in the endocytic pathway. Curr. Opin. Cell Biol. *7*, 552–563.

He, G., Gupta, S., Michaely, P., Hobbs, H.H., and Cohen, J.C. (2002). ARH is a modular adaptor protein that interacts with the LDL receptor, clathrin and AP-2. J. Biol. Chem. *277*, 44044–44049.

Hopkins, C.R., Gibson, A., Shipman, M., Strickland, D.K., and Trowbridge, I.S. (1994). In migrating fibroblasts, recycling receptors are concentrated in narrow tubules in the pericentriolar area, and then routed to the plasma membrane of the leading lamella. J. Cell Biol. *125*, 1265–1274.

Hopkins, C.R., and Trowbridge, I.S. (1983). Internalization and processing of transferrin and the transferrin receptor in human carcinoma A431 cells. J. Cell Biol. *97*, 508–521.

Hung, A.Y., and Sheng, M. (2002). PDZ domains: structural modules for protein complex assembly. J. Biol. Chem. *277*, 5699–5702.

Kerjaschki, D., and Farquhar, M.G. (1983). Immunocytochemical localization of the Heymann nephritis antigen (GP330) in glomerular epithelial cells of normal Lewis rats. J. Exp. Med. *157*, 667–686.

Kerjaschki, D., Noronha-Blob, L., Sacktor, B., and Farquhar, M.G. (1984). Microdomains of distinctive glycoprotein composition in the kidney proximal tubule brush border. J. Cell Biol. *98*, 1505–1513.

Kirchhausen, T. (2002). Clathrin adaptors really adapt. Cell *109*, 413–416.

Lavoie, C., Meerloo, T., Lin, P., and Farquhar, M.G. (2002). Calnuc, an EF-hand Ca(2+)-binding protein, is stored and processed in the Golgi and secreted by the constitutive-like pathway in AtT20 cells. Mol. Endocrinol. *16*, 2462–2474.

Lou, X., McQuistan, T., Orlando, R.A., and Farquhar, M.G. (2002). GAIP, GIPC and Galphai3 are concentrated in endocytic compartments of proximal tubule cells: putative role in regulating megalin's function. J. Am. Soc. Nephrol. *13*, 918–927.

Lundstrom, M., Orlando, R.A., Saedi, M.S., Woodward, L., Kurihara, H., and Farquhar, M.G. (1993). Immunocytochemical and biochemical characterization of the Heymann nephritis antigenic complex in rat L2 yolk sac cells. Am. J. Pathol. *143*, 1423–1435.

Mammoto, A., Ohtsuka, T., Hotta, I., Sasaki, T., and Takai, Y. (1999). Rab11BP/Rabphilin-11, a downstream target of rab11 small G protein implicated in vesicle recycling. J. Biol. Chem. *274*, 25517–25524.

Matteoni, R., and Kreis, T.E. (1987). Translocation and clustering of endosomes and lysosomes depends on microtubules. J. Cell Biol. *105*, 1253–1265.

May, P., Bock, H.H., and Herz, J. (2003). Integration of endocytosis and signal transduction by lipoprotein receptors. Sci. STKE 2003, PE12.

McCarthy, R.A., Barth, J.L., Chintalapudi, M.R., Knaak, C., and Argraves, W.S. (2002). Megalin functions as an endocytic sonic hedgehog receptor. J. Biol. Chem. *277*, 25660–25667.

Miettinen, A., Dekan, G., and Farquhar, M.G. (1990). Monoclonal antibodies against membrane proteins of the rat glomerulus. Immunochemical specificity and immunofluorescence distribution of the antigens. Am. J. Pathol. *137*, 929–944.

Mishra, S.K., Keyel, P.A., Hawryluk, M.J., Agostinelli, N.R., Watkins, S.C., and Traub, L.M. (2002a). Disabled-2 exhibits the properties of a cargo-selective endocytic clathrin adaptor. EMBO J. *21*, 4915–4926.

Mishra, S.K., Watkins, S.C., and Traub, L.M. (2002b). The autosomal recessive hypercholesterolemia (ARH) protein interfaces directly with the clathrin-coat machinery. Proc. Natl. Acad. Sci. USA *99*, 16099–16104.

Morris, S.M., and Cooper, J.A. (2001). Disabled-2 colocalizes with the LDLR in clathrin-coated pits and interacts with AP-2. Traffic *2*, 111–123.

Morris, S.M., Tallquist, M.D., Rock, C.O., and Cooper, J.A. (2002). Dual roles for the Dab2 adaptor protein in embryonic development and kidney transport. EMBO J. *21*, 1555–1564.

Nagai, M., Meerloo, T., Takeda, T., and Farquhar, M.G. (2003). The adaptor protein ARH escorts megalin through recycling dense apical tubules in proximal tubule cells [abstract]. J. Am. Soc. Nephrol. (in press).

Nourry, C., Grant, S.G., and Borg, J.P. (2003). PDZ domain proteins: plug and play! Sci. STKE *2003*, RE7.

Nykjaer, A., Dragun, D., Walther, D., Vorum, H., Jacobsen, C., Herz, J., Melsen, F., Christensen, E.I., and Willnow, T.E. (1999). An endocytic pathway essential for renal uptake and activation of the steroid 25-(OH) vitamin D3. Cell *96*, 507–515.

Oleinikov, A.V., Zhao, J., and Makker, S.P. (2000). Cytosolic adaptor protein Dab2 is an intracellular ligand of endocytic receptor gp600/megalin. Biochem. J. 347, 613–621.

Orlando, R.A., Rader, K., Authier, F., Yamazaki, H., Posner, B.I., Bergeron, J.J., and Farquhar, M.G. (1998). Megalin is an endocytic receptor for insulin. J. Am. Soc. Nephrol. *9*, 1759–1766.

Patrie, K.M., Drescher, A.J., Goyal, M., Wiggins, R.C., and Margolis, B. (2001). The membrane-associated guanylate kinase protein MAGI-1 binds megalin and is present in glomerular podocytes. J. Am. Soc. Nephrol. *12*, 667–677.

Petersen, H.H., Hilpert, J., Militz, D., Zandler, V., Jacobsen, C., Roebroek, A.J., and Willnow, T.E. (2003). Functional interaction of megalin with the megalin-binding protein (MegBP), a novel tetratrico peptide repeat-containing adaptor molecule. J. Cell Sci. *116*, 453–461.

Prekeris, R., Klumperman, J., Chen, Y.A., and Scheller, R.H. (1998). Syntaxin 13 mediates cycling of plasma membrane proteins via tubulovesicular recycling endosomes. J. Cell Biol. *143*, 957–971.

Rader, K., Orlando, R.A., Lou, X., and Farquhar, M.G. (2000). Characterization of ANKRA, a novel ankyrin repeat protein that interacts with the cytoplasmic domain of megalin. J. Am. Soc. Nephrol. *11*, 2167–2178.

Sachse, M., Ramm, G., Strous, G., and Klumperman, J. (2002). Endosomes: multipurpose designs for integrating housekeeping and specialized tasks. Histochem. Cell Biol. *117*, 91–104.

Saito, A., Pietromonaco, S., Loo, A.K., and Farquhar, M.G. (1994). Complete cloning and sequencing of rat gp330/"megalin," a distinctive member of the low density lipoprotein receptor gene family. Proc. Natl. Acad. Sci. USA *91*, 9725–9729.

Sonnichsen, B., De Renzis, S., Nielsen, E., Rietdorf, J., and Zerial, M. (2000). Distinct membrane domains on endosomes in the recycling pathway visualized by multicolor imaging of Rab4, Rab5, and Rab11. J. Cell Biol. *149*, 901–914.

Takeda, T., McQuistan, T., Orlando, R.A., and Farquhar, M.G. (2001). Loss of glomerular foot processes is associated with uncoupling of podocalyxin from the actin cytoskeleton. J. Clin. Investig. *108*, 289–301.

Takeda, T., Yamazaki, H., and Farquhar, M.G. (2003). Identification of an Apical Sorting Determinant in the Cytoplasmic Tail of Megalin. Am. J. Physiol. *284*, C1105–C1113.

Trischler, M., Stoorvogel, W., and Ullrich, O. (1999). Biochemical analysis of distinct Rab5- and Rab11-positive endosomes along the transferrin pathway. J. Cell Sci. *112*, 4773–4783.

Ullrich, O., Reinsch, S., Urbe, S., Zerial, M., and Parton, R.G. (1996). Rab11 regulates recycling through the pericentriolar recycling endosome. J. Cell Biol. *135*, 913–924.

Velasco, A., Hendricks, L., Moremen, K.W., Tulsiani, D.R., Touster, O., and Farquhar, M.G. (1993). Cell type-dependent variations in the subcellular distribution of alpha-mannosidase I and II. J. Cell Biol. *122*, 39–51.

Willnow, T.E., Hilpert, J., Armstrong, S.A., Rohlmann, A., Hammer, R.E., Burns, D.K., and Herz, J. (1996). Defective forebrain development in mice lacking gp330/megalin. Proc. Natl. Acad. Sci. USA *93*, 8460–8464.

Yamashiro, D.J., Tycko, B., Fluss, S.R., and Maxfield, F.R. (1984). Segregation of transferrin to a mildly acidic (pH 6.5) para-Golgi compartment in the recycling pathway. Cell *37*, 789–800.

Yamazaki, H., Ullrich, R., Exner, M., Saito, A., Orlando, R.A., Kerjaschki, D., and Farquhar, M.G. (1998). All four putative ligand-binding domains in megalin contain pathogenic epitopes capable of inducing passive Heymann nephritis. J. Am. Soc. Nephrol. *9*, 1638–1644.

Yan, K.S., Kuti, M., and Zhou, M.M. (2002). PTB or not PTB – that is the question. FEBS Lett *513*, 67–70.

Zheng, G., Bachinsky, D.R., Stamenkovic, I., Strickland, D.K., Brown, D., Andres, G., and McCluskey, R.T. (1994). Organ distribution in rats of two members of the low-density lipoprotein receptor gene family, gp330 and LRP/alpha 2MR, and the receptor-associated protein (RAP). J. Histochem. Cytochem. *42*, 531–542.